Myocardial Viability Index in Chronic Coronary Artery Disease: Technetium-99m-Methoxy Isobutyl Isonitrile Redistribution

Simone Maurea, Alberto Cuocolo, Andrea Soricelli, Luisa Castelli, Fiorenzo Squame, Massimo Imbriaco, Nicola De Luca, Bruno Trimarco and Marco Salvatore

Nuclear Medicine Department, CNR Nuclear Medicine Center and Medical Clinic, University Federico II; and National Cancer Institute, Naples, Italy

The purpose of this study was to evaluate whether an additional redistribution image after a rest ^{99m}Tc-MIBI injection enhances detection of viable myocardium and predicts functional recovery after coronary revascularization in patients with chronic coronary artery disease (CAD). **Methods:** Thirty-one patients (29 men, mean age 55 ± 10 yr) with proven CAD and left ventricular (LV) dysfunction (ejection fraction 39% ± 9%) underwent resting ^{99m}Tc-MIBI tomography with initial (1 hr) and delayed (5 hr) images. Within 1 wk of MIBI imaging, all patients underwent rest-redistribution ^{201}Tl imaging. Eight patients also underwent two-dimensional echocardiography before and 5 ± 3 mo after coronary revascularization. **Results:** On the initial ^{99m}Tc-MIBI images, 302 myocardial segments were normal, 183 showed moderate and 197 severe reduction of tracer uptake. Of these 197 segments, 47 (24%) demonstrated increased tracer uptake (≥10% versus initial) on delayed images (from 43% ± 8% to 60% ± 8%, $p<0.001$) and were considered as showing ^{99m}Tc-MIBI redistribution. These 47 segments were observed in 20 (65%) patients in whom ^{201}Tl images detected viable myocardium in the same segments. In the eight patients studied before and after revascularization, 83% of segments with ^{99m}Tc-MIBI redistribution and abnormal LV function showed functional recovery after revascularization, while 96% of segments without ^{99m}Tc-MIBI redistribution did not show functional recovery. **Conclusion:** Resting ^{99m}Tc-MIBI redistribution frequently occurs in patients with chronic CAD. Acquisition of ^{99m}Tc-MIBI redistribution images enhances detection of viable myocardium and predicts functional recovery after revascularization.

Key Words: technetium-99m-sestamibi; left ventricular dysfunction; functional recovery; thallium-201

J Nucl Med 1995; 36:1953–1960

Technetium-99m-methoxy isobutyl isonitrile (MIBI) is a cardiac perfusion agent that initially distributes in the myocardium proportional to coronary blood flow, similar to ^{201}Tl (*1,2*). It has been suggested that ^{99m}Tc-MIBI does not show significant redistribution (*1*). Recent studies, however, demonstrated that delayed ^{99m}Tc-MIBI redistribution may be observed in a model of transient myocardial ischemia (*3*) or under conditions of sustained low coronary flow (*4*). Furthermore, it has also been reported that myocardial uptake and retention of ^{99m}Tc-MIBI are dependent on both cell viability and regional blood flow and that tissue viability is required for ^{99m}Tc-MIBI redistribution (*5–9*).

Clinical studies evaluated the phenomenon of ^{99m}Tc-MIBI redistribution after stress injection in patients with CAD (*10,11*). The occurrence of ^{99m}Tc-MIBI redistribution after rest injection and its clinical implications have not yet been widely evaluated. Preliminary results reported by Dilsizian et al. recently suggested that ^{99m}Tc-MIBI redistribution imaging following tracer injection at rest can detect viable myocardium using standard imaging protocols (*12*). Furthermore, these authors suggest that detection of viable myocardium may be enhanced with ^{99m}Tc-MIBI cardiac imaging if an additional redistribution image is acquired after tracer injection at rest (*12*). It is still uncertain, however, whether ^{99m}Tc-MIBI redistribution after rest injection is predictive of improved ventricular function after coronary revascularization.

The purpose of this study was to evaluate whether an additional redistribution image after rest ^{99m}Tc-MIBI injection enhances detection of viable myocardium and predicts functional recovery after coronary revascularization in patients with chronic coronary artery disease (CAD).

MATERIALS AND METHODS

Patients

We prospectively studied 31 patients (29 men, 2 women; mean age 55 ± 10 yr) with angiographically documented CAD and with left ventricular dysfunction (Tables 1 and 2). Seven patients had significant stenosis of all three major coronary vessels, 11 had significant stenosis of two major coronary vessels and 13 had significant stenosis of only one major coronary vessel. The mean left ventricular ejection fraction (LVEF) by resting equilibrium radionuclide angiography was 39% ± 9%. All patients had a previous myocardial infarction that was documented clinically and by electrocardiography. No patient, however, had an acute myocardial infarction within 6 mo of the study. The majority of patients

Received Jan. 1, 1995; revision accepted Jul. 14, 1995
For correspondence or reprints contact: Simone Maurea, MD, via Raffaele De Cesare 7, 80132 Napoli, Italy.

TABLE 1
Patient Characteristics

Patient no.	Sex	Age (yr)	LVEF (%)	Site of myocardial infarction	Stable angina
1	M	62	42	Posterolateral	Yes
2	M	62	24	Inferior, anterior	Yes
3	M	44	49	Anteroseptal	Yes
4	M	63	38	Anterior	Yes
5	M	57	44	Inferior	Yes
6	M	67	42	Inferior	Yes
7	M	60	39	Inferolateral	Yes
8	M	49	35	Anteroseptal, inferoapical	No
9	M	69	39	Inferolateral	Yes
10	M	46	34	Anterior	Yes
11	M	63	48	Inferolateral	Yes
12	M	48	28	Anterior	Yes
13	M	43	41	Anteroseptal	Yes
14	M	61	42	Inferior, anterior	Yes
15	M	40	48	Anteroseptal	Yes
16	M	63	31	Anteroseptal, inferior	Yes
17	M	54	30	Inferolateral	Yes
18	M	66	47	Anteroapical	Yes
19	M	58	49	Inferior	Yes
20	M	65	48	Anterior	Yes
21	M	61	30	Anterior	Yes
22	M	68	49	Anterior	Yes
23	M	50	36	Anteroseptal	Yes
24	M	57	48	Anteroseptal, apical	Yes
25	M	38	23	Anterior	No
26	M	32	26	Anterior, inferior	No
27	M	42	20	Anterior	Yes
28	M	53	49	Anterior	Yes
29	M	47	44	Anterolateral	Yes
30	F	57	46	Inferior	Yes
31	F	65	44	Anterior	Yes

LVEF = left ventricular ejection fraction.

(n = 28) were symptomatic with episodes of stable angina requiring antianginal treatment, while three patients were asymptomatic. All patients, however, underwent radionuclide studies after withdrawal of all medications. Eight of the 31 patients were also studied after coronary revascularization, coronary artery bypass graft in six and percutaneous transluminal coronary angioplasty in two. In these patients, none had clinical evidence of perioperative or postangioplasty myocardial infarction or restenosis. Informed consent, as part of the protocol approved by the Institutional Clinical Research Subpanel on Human Studies at our University, was obtained from all patients.

Technetium-99m-MIBI Imaging

After an overnight fast, all patients underwent rest-redistribution ^{99m}Tc-MIBI myocardial tomography. Patients were ambulatory and remained in the resting condition for 30 min before intravenous injection of ^{99m}Tc-MIBI (740 MBq). Initial images were acquired 1 hr after tracer administration. Delayed images were then taken 5 hr later.

SPECT was performed as previously described (*13*) using a rotating large field of view gamma camera equipped with a low-energy, all-purpose, parallel-hole collimator and connected with a dedicated computer system. Briefly, 32 projections (40 sec/projection) were obtained over a semicircular 180° arch, which extended from the 30° right anterior oblique to the left posterior oblique position. A 20% symmetric energy window centered on the 140-keV peak was used. All projection images were stored on magnetic disk in a 64 × 64 word matrix. Each projection image was corrected for nonuniformity, with a 120-million count image obtained weekly from a uniform ^{57}C flood source. The mechanical center of rotation was determined from the projection data to align the detector data with respect to the reconstruction matrix (*14*). The raw data were initially smoothed with a nine-point weighted average algorithm. Filtered backprojection was then performed with a low-resolution Butterworth filter with a cutoff frequency of 0.5 cycles/pixel, order 5.0, to reconstruct transverse axial tomograms of 6.2-mm thickness per slice, which encompassed the entire heart. Sagittal and oblique tomograms parallel to the long-axis and short-axis of the left ventricle were then extracted from the filtered transaxial tomograms by performing coordinate transformation with the appropriate interpolation (*14*). No attenuation or scatter correction was applied.

Thallium-201 Imaging

All patients underwent rest-redistribution ^{201}Tl myocardial tomography. Patients were ambulatory and remained in the resting condition for 30 min before thallium administration. After an overnight fast, ^{201}Tl (111 MBq) was intravenously injected at rest. Initial and delayed images were acquired 15 min and 4 hr after injection. During the time between the initial and delayed images, all patients were ambulatory and remained in the fasting state. A 3-day interval separated the thallium from ^{99m}Tc-MIBI study. SPECT acquisition was performed with the same gamma camera, matrix and computer system used for the ^{99m}Tc-MIBI studies. The photopeak was centered on the 68-keV with a 20% window.

Echocardiography

During the same week of ^{99m}Tc-MIBI and ^{201}Tl imaging, all patients underwent echocardiographic studies. A phased-array sector scanner with a 2.5 MHz transducer was used. Two-dimensional images of the left ventricle were obtained at rest with the patient lying in the left lateral decubitus position using multiple imaging sections, including the parasternal long- and short-axes and apical two- and four-chamber views. Images were recorded on videotape for analysis. In the eight patients studied before and after coronary revascularization, two sequential echocardiographic studies were performed. The first evaluation (baseline) was performed during the same week of ^{99m}Tc-MIBI and ^{201}Tl studies. The second evaluation (follow-up) was performed an average of 5 ± 3 mo after coronary revascularization. No patient received beta-blockers or inotropic drugs during the follow-up evaluation.

Data Analysis

In each patient, corresponding initial and delayed ^{99m}Tc-MIBI and rest-redistribution ^{201}Tl tomographic images were evaluated for direct comparison, as previously described (*13*). For each study, tomograms were divided into 22 myocardial segments (Fig. 1). Regional ^{99m}Tc-MIBI and ^{201}Tl uptake were quantitatively analyzed. In each tomogram, the myocardial region with the maximum counts was considered as the normal reference region. Technetium-99m-MIBI and ^{201}Tl uptake in all other segments were then expressed as the percentage of the activity measured in the reference region.

To assess the normal range for quantitative data analysis, a group of 14 age-matched normal volunteers (13 men, 1 woman) with no evidence of cardiovascular or pulmonary disease was also studied. In these subjects, clinical examination, echocardiograms and stress electrocardiograms were normal. A myocardial segment

TABLE 2
Angiographic Data, Site of Left Ventricular Dysfunction and Technetium-99m-MIBI Redistribution on Delayed Imaging

Patient no.	Coronary artery stenosis (≥50%)	Site of wall motion abnormalities	Site of Segments with ^{99m}Tc-MIBI redistribution
1	LAD, LCx, PDA	Lateral	Lateral, inferoseptal, apical (n = 4)
2	LAD, PDA	Inferior, apical	Inferoseptal, anteroseptal (n = 2)
3	LAD, LCx	Septal, apical	Anteroseptal, apical, inferior (n = 8)
4	LAD, LCx, PDA	Septal, lateral, apical	Inferoseptal, inferolateral, apical (n = 3)
5	PDA	Inferolateral	Inferolateral, septal (n = 5)
6	LAD, PDA	Inferior	None
7	LAD, LCx	Septal, inferoapical, lateral	Apical (n = 1)
8	LAD	Inferoapical	Apical (n = 1)
9	LAD, LCx, PDA	Septal, posterolateral	Inferoseptal (n = 1)
10	LAD, PDA	Anteroapical	Inferolateral, anterior (n = 2)
11	LAD, PDA	Septal, inferolateral	Lateral (n = 1)
12	LCx	Anteroseptal, apical	Anteroseptal, inferolateral (n = 5)
13	LAD, LCx	Septal	None
14	LAD, LCx, PDA	Inferoapical	Inferolateral (n = 1)
15	LAD	Septal	None
16	LAD, LCx, PDA	Anteroseptal, apical	Apical (n = 1)
17	LAD, PDA	Inferoapical	None
18	LAD	Anterior, apical	None
19	PDA	Inferoapical	None
20	LAD, LCx	Anteroseptal	None
21	LAD	Anteroapical, inferior	Anteroseptal, apical (n = 4)
22	LAD, LCx, PDA	Septal	None
23	LAD	Septal	None
24	LAD	Apical	None
25	LAD	Anterior, inferoapical	Inferoseptal (n = 1)
26	LAD, LCx	Anterior, inferior, apical	None
27	LAD	Anterior, apical	Septal (n = 1)
28	LCx, PDA	Septal	Inferoseptal (n = 1)
29	LAD	Anteroseptal	Inferoseptal, inferolateral (n = 3)
30	LAD, LCx, PDA	Inferoapical, septal	Inferolateral (n = 1)
31	LAD	Anteroseptal, apical	Apical (n = 1)

LAD = left anterior descending artery; LCx = left circumflex artery; PDA = posterior descending artery.

was considered abnormal if initial ^{99m}Tc-MIBI or ^{201}Tl uptake was >2 s.d. below the mean observed in the same region for age- and sex-matched normal volunteers. On initial ^{99m}Tc-MIBI images, segments with abnormal uptake were subgrouped on the basis of severity of reduction in tracer activity: moderate (≥50% of peak activity) and severe (<50% of peak) defects, as previously reported (*12,15,16*). On the basis of previous reproducibility measurements performed by other authors and in our laboratory (*12,17*), a segment with reduced activity on initial ^{99m}Tc-MIBI or ^{201}Tl images was considered reversible if the activity increased ≥10% on delayed ^{99m}Tc-MIBI or ^{201}Tl images, respectively. Alternatively, a segment with reduced activity on initial ^{99m}Tc-MIBI or ^{201}Tl images was considered irreversible if the activity did not increase ≥10% or increased ≥10% but remained <50% on delayed ^{99m}Tc-MIBI or ^{201}Tl images, respectively. Thallium-201 irreversible defects were divided on the basis of severity of reduction in tracer activity: moderate (≥50% of peak activity) and severe (<50% of peak) defects, as previously reported (*12,17*).

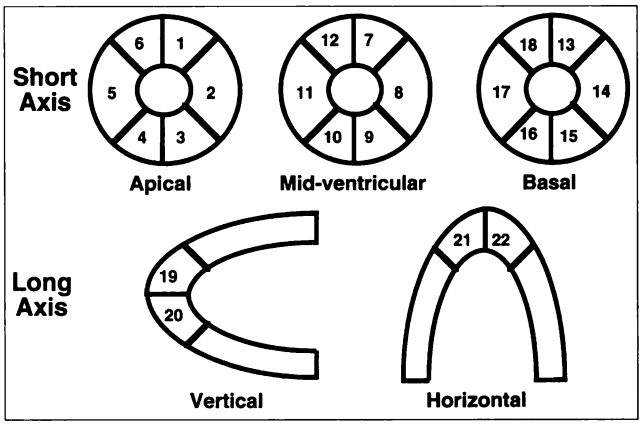

FIGURE 1. Diagram of standard segmentation scheme used for regional quantitative analysis of ^{99m}Tc-MIBI and ^{201}Tl uptake.

Echocardiographic images were interpreted by two experienced observers who were unaware of clinical, radionuclide and angiographic findings. A third investigator blindly reviewed the echocardiograms when the first two observers did not agree. Regional left ventricular function was assessed according to the recommendations of the American Society of Echocardiography (*18,19*). Segmental left ventricular wall motion was graded as: 1, normal; 2, hypokinetic; 3, akinetic; and 4, dyskinetic. The echocardiographic

results were directly compared with those of ^{99m}Tc-MIBI and ^{201}Tl, as previously described (*20*). In the eight patients studied before and after coronary revascularization, a myocardial segment was considered as showing functional recovery when the regional wall motion score was abnormal at baseline and improved at least one echocardiographic grade during the follow-up study, as previously reported (*21*). Conversely, a myocardial segment was considered as showing no functional recovery when regional wall motion score was severely impaired at baseline (grade 3 or 4) and did not change during follow-up (*21*).

Statistical Analysis

Data are expressed as mean ± 1 s.d. Differences in the mean values were assessed by Student's t-test for unpaired data with Bonferroni correction for multiple groups comparison, or Student's t test for paired data, as appropriate. Bonferroni correction establishes that the p value for each comparison should be multiplied by the total number of comparisons undertaken (*22*). The Spearman correlation coefficient (ρ) was used to assess the relationships between wall motion score and tracer uptake. Linear regression was used to evaluate the relationship between LVEF and the number of myocardial segments showing reversible ^{99m}Tc-MIBI defects. Chi square analysis was used to assess differences between proportions. Probability values <0.05 were considered significant.

RESULTS

Technetium-99m-MIBI

A total of 682 myocardial segments were analyzed. On initial ^{99m}Tc-MIBI images, 302 (44%) segments had normal tracer uptake, 183 (27%) showed moderate and 197 (29%) severe reduction of tracer uptake.

Myocardial segments with moderate reduction of ^{99m}Tc-MIBI uptake on the initial images were observed in all 31 patients (range 3–10 segments/patient, mean 5.9 ± 1.9). Of the 183 segments with moderate reduction of ^{99m}Tc-MIBI uptake on initial images, 51 (28%) were reversible on delayed images, showing significant increased tracer uptake (from 61% ± 7% to 78% ± 10% of peak activity, $p<0.001$). Moderate reversible ^{99m}Tc-MIBI defects on delayed images were observed in 23 (74%) patients (range 1–5 segments/patient, mean 2.2 ± 1.2). The remaining 132 (72%) segments with moderate reduction of ^{99m}Tc-MIBI uptake on initial images were irreversible on delayed images, showing no significant change in tracer uptake (from 63% ± 6% to 58% ± 9% of peak activity).

Myocardial segments with severe reduction of ^{99m}Tc-MIBI uptake on initial images were observed in all 31 patients (range 1–14 segments/patient, mean 6.4 ± 3.6). Of the 197 segments with severe reduction of ^{99m}Tc-MIBI uptake on initial images, 47 (24%) were reversible on delayed images, showing significant increased tracer uptake (from 43% ± 8% to 60% ± 8% of peak activity, $p<0.001$) (Fig. 2). Severe reversible ^{99m}Tc-MIBI defects on delayed images were observed in 20 (65%) patients (range 1–8 segments/patient, mean 2.3 ± 1.9) (Table 2). The remaining 150 (76%) segments with severe reduction of ^{99m}Tc-MIBI uptake on the initial images were irreversible on delayed images, showing no significant change in tracer uptake (from 33% ± 12% to 32% ± 12% of peak activity) (Fig. 3). In particular, reversible severe ^{99m}Tc-MIBI defects showed significantly higher tracer uptake on initial images compared to irreversible ^{99m}Tc-MIBI defects (43% ± 8% versus 33% ± 12%, $p<0.001$).

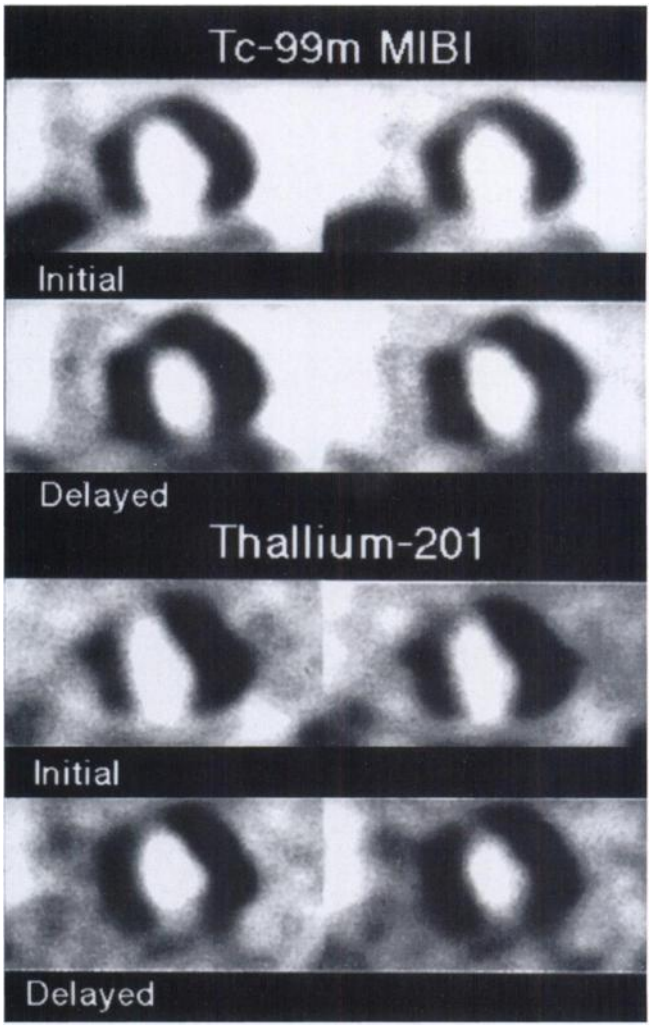

FIGURE 2. Technetium-99m-MIBI cardiac imaging under resting conditions: short-axis slices show a reversible defect involving the septal region (top). Corresponding rest-redistribution ^{201}Tl cardiac tomography: short-axis slices show a reversible defect involving the septal region (bottom).

Thallium-201

Of the 51 myocardial segments with moderate reversible ^{99m}Tc-MIBI defects, 17 had normal thallium uptake, 19 showed reversible and 15 moderate irreversible thallium defects. None of the 132 segments with moderate irreversible ^{99m}Tc-MIBI defects showed severe irreversible thallium defects. In particular, 28 had normal thallium uptake, 31 showed reversible and 73 moderate irreversible thallium defects.

None of the 47 myocardial segments with severe reversible ^{99m}Tc-MIBI defects showed severe irreversible ^{201}Tl defects. In particular, 3 of these segments had normal thallium uptake, 22 showed reversible and 22 moderate

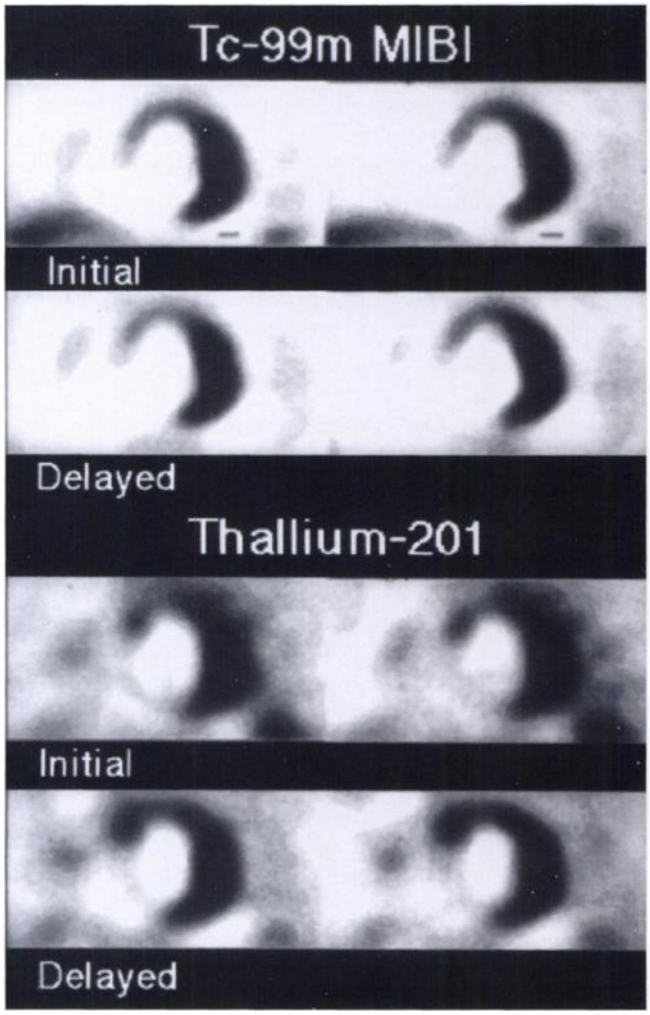

FIGURE 3. Technetium-99m-MIBI cardiac tomography under resting conditions: short-axis slices show a large irreversible defect involving the septal and inferior regions (top). Corresponding rest-redistribution ^{201}Tl cardiac tomography: short-axis slices show a large irreversible defect involving the septal and inferior regions (bottom).

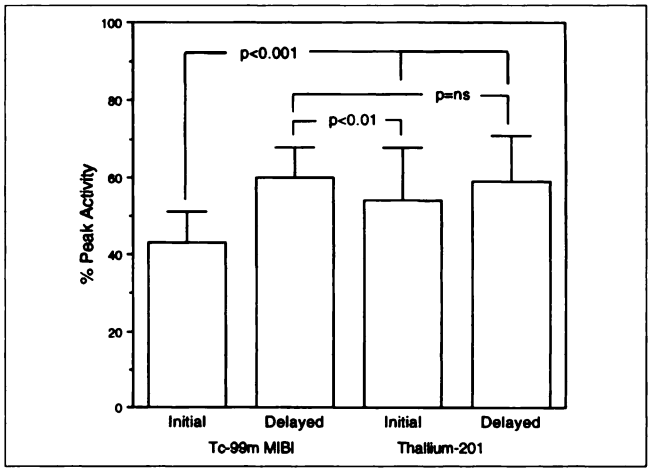

FIGURE 4. Technetium-99m-MIBI and ^{201}Tl uptake (expressed as percentage of peak activity) in myocardial segments with severe reduction of initial ^{99m}Tc-MIBI uptake and increased tracer uptake on delayed images. ns = nonsignificant.

irreversible thallium defects (Fig. 2). On the other hand, the majority (80%) of myocardial segments with severe irreversible ^{99m}Tc-MIBI defects showed severe irreversible ^{201}Tl defects (Fig. 3).

In the 47 myocardial segments with severe reversible ^{99m}Tc-MIBI defects, initial ^{99m}Tc-MIBI uptake was significantly lower ($p<0.001$) compared to both initial and delayed thallium uptake (Fig. 4). On the other hand, in these segments delayed ^{99m}Tc-MIBI uptake was significantly higher ($p<0.01$) compared to initial thallium uptake, but not different from delayed thallium uptake (Fig. 4).

Relation with Left Ventricular Function

Of the total 682 myocardial segments, 332 (49%) showed normal wall motion (Group 1) on echocardiographic images, 160 (23%) were hypokinetic (Group 2) and 190 (28%) were akinetic or dyskinetic (Group 3). Initial and delayed thallium uptake were significantly higher ($p<0.001$) for Group 1 in segments compared with those of Groups 2 and 3 and in Group 2 segments compared to those of Group 3 (Table 3). Similarly, initial and delayed ^{99m}Tc-MIBI uptake were significantly higher ($p<0.001$) in Group 1 segments compared with those of Groups 2 and 3 and in Group 2 segments compared to those of Group 3 (Table 3). A significant relationship ($p<0.001$) between wall motion score and initial ($\rho = -0.45$) and delayed ($\rho = -0.41$) thallium uptake was observed. Similarly, a significant relationship ($p<0.001$) between wall motion score and initial ($\rho = -0.50$) and delayed ($\rho = -0.47$) ^{99m}Tc-MIBI uptake was found. No significant relationship was observed between LVEF and the number of myocardial segments showing moderate and/or severe reversible ^{99m}Tc-MIBI defects.

Follow-up after Coronary Revascularization

In the eight patients studied before and after coronary revascularization, 33 (19%) myocardial segments with wall motion abnormalities showed moderate reduction of ^{99m}Tc-MIBI uptake on initial images. Of these 33 segments, 13 were reversible and 20 did not change on delayed ^{99m}Tc-MIBI images. Moderate reversible ^{99m}Tc-MIBI defects on

TABLE 3.
Initial and Delayed Technetium-99m-MIBI and Thallium-201 Uptake in Myocardial Segments*

	Group 1	Group 2	Group 3
Myocardial segments (no.)	332	160	190
Initial ^{99m}Tc-MIBI uptake (%)	89 ± 13	60 ± 11†	38 ± 16‡
Delayed ^{99m}Tc-MIBI uptake (%)	87 ± 14	62 ± 14†	39 ± 18‡
Initial ^{201}Tl uptake (%)	88 ± 14	65 ± 14†	42 ± 20‡
Delayed ^{201}Tl uptake (%)	87 ± 15	67 ± 14†	45 ± 21‡

*Group 1 = normal wall motion; Group 2 = hypokinetic segments; Group 3 = segments with akinesia or dyskinesia.
†$p < 0.001$ versus Group 1; ‡$p < 0.001$ versus Groups 1 and 2.

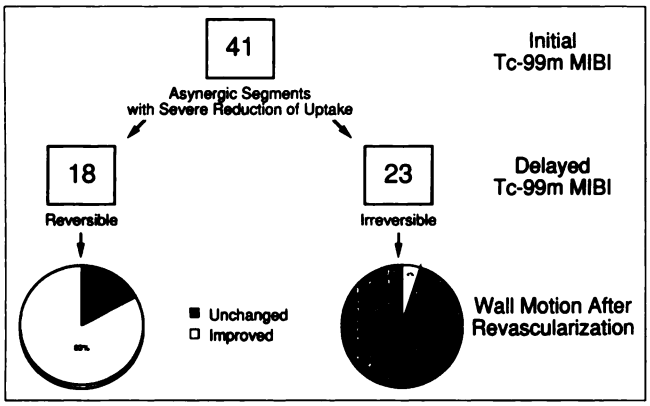

FIGURE 5. Flow diagram shows wall motion after coronary revascularization in asynergic segments with severe reduction of ^{99m}Tc-MIBI uptake on initial images and reversible or irreversible defects on delayed images.

delayed images were observed in seven of these patients (range 0–4 segments/patient, mean 2.1 ± 1.4). The majority of segments with moderate reversible ^{99m}Tc-MIBI defects (85%) showed functional recovery after revascularization. Furthermore, 41 (23%) segments with wall motion abnormalities showed severe reduction of ^{99m}Tc-MIBI uptake on initial images. Of these 41 segments, 18 were reversible and 23 did not change on delayed ^{99m}Tc-MIBI images. Severe reversible ^{99m}Tc-MIBI defects on delayed images were observed in all these patients (range 1–8 segments/patient, mean 3.1 ± 2.6). The majority (83%) of segments with severe reversible ^{99m}Tc-MIBI defects showed functional recovery after revascularization (Fig. 5). Conversely, the majority (96%) of segments with severe irreversible ^{99m}Tc-MIBI defects did not show improved wall motion after revascularization ($p<0.001$ versus severe reversible defects) (Fig. 5). In these patients, LVEF significantly ($p<0.01$) improved after revascularization (from 42% ± 7% at baseline to 47% ± 7% after revascularization).

DISCUSSION

Our results agree with those of Dilsizian et al. (*12*) and demonstrate that in patients with chronic CAD and left ventricular dysfunction ^{99m}Tc-MIBI redistribution on delayed images occurs in 24% to 38% of myocardial segments with severe reduction of tracer uptake at rest. Delayed ^{99m}Tc-MIBI imaging improves the differentiation between ischemic but still viable myocardium from fibrotic tissue in regions with severe reduction of resting ^{99m}Tc-MIBI uptake. Furthermore, ^{99m}Tc-MIBI redistribution is predictive of functional recovery following coronary revascularization.

Technetium-99m-MIBI Identification of Myocardial Viability

Previous clinical studies demonstrated that severe reduction of ^{99m}Tc-MIBI uptake underestimates the presence of viable myocardium in patients with chronic CAD and left ventricular dysfunction (*12,15,16,23–31*). In particular, comparative studies between ^{99m}Tc-MIBI scintigraphy and metabolic imaging with [^{18}F] fluorodeoxyglucose showed that ^{99m}Tc-MIBI myocardial uptake on conventional 1-hr imaging is mainly related to regional coronary blood flow rather than tissue viability (*15,31*). Experimental studies, however, have shown that myocardial retention of ^{99m}Tc-MIBI depends not only on coronary blood flow but also on cellular viability (*5,6*). Furthermore, recent clinical reports suggest that quantitative analysis of resting ^{99m}Tc-MIBI may enhance differentiation between viable myocardium from necrotic tissue in patients with chronic ischemic left ventricular dysfunction (*12,32*).

Technetium-99m-MIBI Redistribution

The occurrence of ^{99m}Tc-MIBI redistribution has been previously demonstrated in a model of transient ischemia or under conditions of sustained reduced coronary blood flow (*3,4*). In particular, Li et al. showed that normalization of ^{99m}Tc-MIBI defects in ischemic regions is progressive over time and that such redistribution is detectable on tomographic images and also confirmed by serial myocardial biopsies (*3*). Sinusas et al. recently demonstrated that ^{99m}Tc-MIBI redistributes in the presence of severe coronary artery stenosis, as documented by gamma well counting techniques and by high-resolution postmortem gamma camera imaging of myocardial slices (*4*). In clinical studies, there are conflicting data on ^{99m}Tc-MIBI redistribution after stress imaging. Taillefer et al. (*10*) described a decrease in ^{99m}Tc-MIBI defect size after exercise with serial planar imaging between 1 hr and 3 hr following stress injection. On the other hand, Villanueva-Meyer et al. (*11*) recently reported no change in defect size between 1 and 4 hr after stress ^{99m}Tc-MIBI injection using quantitative tomographic imaging. Dilsizian et al. recently described redistribution of ^{99m}Tc-MIBI after rest injection in a small number of patients with chronic CAD and severe left ventricular dysfunction (*12*). Its clinical utility, however, has not yet gained wide application.

The results of the present study show the occurrence of ^{99m}Tc-MIBI redistribution after rest injection in patients with chronic ischemic left ventricular dysfunction, suggesting that acquisition of delayed images after resting ^{99m}Tc-MIBI injection may enhance the detection of severely hypoperfused but still viable myocardium. We focused our analysis on the clinical significance of ^{99m}Tc-MIBI redistribution in myocardial segments with severe reduction of tracer uptake on initial images, in whom the presence of viable tissue is in question. In particular, 24% of segments with severe reduction of ^{99m}Tc-MIBI uptake on initial images showed a significant increase in tracer uptake on delayed images. Our results with earlier data of Dilsizian et al. in a group of patients with chronic CAD (*12*). These authors described ^{99m}Tc-MIBI redistribution in 38% of myocardial segments with irreversible defects on stress-rest ^{99m}Tc-MIBI imaging (*12*). Furthermore, our results confirm the experimental evidence of resting ^{99m}Tc-MIBI redistribution in a model of sustained coronary low flow (*4*).

In our study, the occurrence of ^{99m}Tc-MIBI redistribution on delayed images in myocardial segments with severe reduction of ^{99m}Tc-MIBI uptake on initial images was observed in 65% of the patients. This finding may be clinically relevant since it demonstrates that ^{99m}Tc-MIBI redistribution may occur in a substantial number of patients with chronic ischemic left ventricular dysfunction.

Comparison with Thallium-201 Imaging

The results of rest-redistribution ^{201}Tl cardiac imaging in myocardial segments with ^{99m}Tc-MIBI redistribution support the hypothesis that these regions may contain hypoperfused but viable myocardium. In particular, each segment showed evidence of myocardial viability according to thallium imaging criteria. In myocardial segments with severe reversible ^{99m}Tc-MIBI defects, initial ^{99m}Tc-MIBI uptake was significantly lower compared to both initial and delayed thallium uptake. A possible explanation for this finding could be that only segments with severe reduction of initial ^{99m}Tc-MIBI uptake and increased tracer activity on delayed images were included in the analysis. Moreover, none of these segments showed severe irreversible thallium defects. On the other hand, delayed ^{99m}Tc-MIBI uptake was significantly higher compared to initial thallium uptake but not different compared to delayed thallium uptake. These data correlate with previous comparative studies between ^{201}Tl and ^{99m}Tc-MIBI cardiac imaging (*26–29*). Furthermore, Dilsizian et al. recently reported concordant results between resting ^{99m}Tc-MIBI redistribution and ^{201}Tl reinjection imaging studies (*12*). These findings suggest that resting ^{99m}Tc-MIBI redistribution imaging identifies the presence of hypoperfused but viable myocardium in patients with chronic ischemic left ventricular dysfunction. Thus, it may have important clinical implications.

Follow-up after Coronary Revascularization

Although thallium uptake is usually considered an accurate marker of myocardial viability in patients with chronic CAD (*33–40*), the definite gold standard for the presence of viable tissue in such patients is functional recovery after coronary revascularization (*41*). In the present study, we evaluated whether resting ^{99m}Tc-MIBI redistribution is predictive of improved left ventricular function after coronary revascularization and, thus, of myocardial viability. Our results obtained after revascularization support the hypothesis that ^{99m}Tc-MIBI redistribution reflects the presence of viable myocardium. In fact, the majority of segments with severely impaired ventricular function and increased ^{99m}Tc-MIBI uptake on delayed images showed improved wall motion after revascularization. Conversely, the majority of akinetic segments with no change on delayed ^{99m}Tc-MIBI images did not show functional recovery after coronary revascularization. Furthermore, a significant improvement of global LVEF was observed after coronary revascularization. Therefore, these findings demonstrate that delayed redistribution cardiac imaging after resting ^{99m}Tc-MIBI injection can detect severely hypoperfused but still viable myocardium as well as predict reversibility of severe regional wall motion abnormalities after coronary revascularization in patients with chronic ischemic left ventricular dysfunction.

Study Limitations

Two potential limitations of this study deserve comment. First, follow-up evaluation after coronary revascularization was obtained in a limited number of the patients in whom resting ^{99m}Tc-MIBI redistribution was observed. Although our data need confirmation in larger series of patients, the follow-up results of the present study confirm and may be considered representative of the enhanced detection of viable myocardium by resting ^{99m}Tc-MIBI cardiac imaging using delayed acquisition. Second, since there are no established criteria in the literature to assess the severity of ^{99m}Tc-MIBI defects, the selection of the threshold value for severely reduced ^{99m}Tc-MIBI uptake was chosen arbitrarily. The same threshold, however, has been used in previous studies (*12,15,16*).

CONCLUSION

Resting ^{99m}Tc-MIBI redistribution frequently occurs in patients with chronic CAD and left ventricular dysfunction. Acquisition of delayed ^{99m}Tc-MIBI images enhances the differentiation between severely hypoperfused, but still viable myocardium from fibrotic tissue in such patients. The presence of ^{99m}Tc-MIBI redistribution may be predictive of functional recovery after coronary revascularization. Therefore, our results suggest that resting ^{99m}Tc-MIBI cardiac imaging should be delayed when assessing myocardial viability in patients with chronic CAD.

REFERENCES

1. Okada RD, Glover D, Gaffney T, Williams S. Myocardial kinetics of technetium-99m-hexakis-2-methoxy-2-methylpropyl-isonitrile. *Circulation* 1988; 77:491–498.
2. Canby RC, Silber S, Pohost GM. Relations of the myocardial imaging agents Tc-99m MIBI and Tl-201 to myocardial blood flow in a canine model of myocardial ischemic insult. *Circulation* 1990;81:289–296.
3. Li QS, Solot A, Frank TL, Wagner HN, Becker LC. Myocardial redistribution of technetium-99m methoxy isobutyl isonitrile (sestamibi). *J Nucl Med* 1990;31:1069–1076.
4. Sinusas AJ, Bergin JD, Edwards NC, et al. Redistribution of Tc-99m sestamibi and Tl-201 in the presence of a severe coronary artery stenosis. *Circulation* 1994;89:2332–2341.
5. Beanlands RSB, Dawood F, Wen WH, et al. Are the kinetics of technetium-99m-methoxyisobutyl isonitrile affected by cell metabolism and viability? *Circulation* 1990;82:1802–1814.
6. Freeman I, Grunwald AM, Hoory S, Bodenheimer MM. Effect of coronary occlusion and myocardial viability on myocardial activity of technetium-99m-sestamibi. *J Nucl Med* 1991;32:292–299.
7. Glover DK, Okada RD. Myocardial technetium-99m sestamibi kinetics after reperfusion in a canine model. *Am Heart J* 1993;125:657–666.
8. Beller GA, Glover DK, Edwards NC, Ruiz M, Simanis JP, Watson DD. Technetium-99m-sestamibi uptake and retention during myocardial ischemia and reperfusion. *Circulation* 1993;87:2033–2042.
9. Merhi J, Arsenault A, Latour JG. Time course of technetium-99m-sestamibi myocardial distribution in dogs with a permanent or transient coronary occlusion. *Eur J Nucl Med* 1994;21:481–487.
10. Taillefer R, Primeau M, Costi P, Lambert R, Leveille J, Latour Y. Technetium-99m-sestamibi myocardial perfusion imaging in detection of coronary artery disease: comparison between initial (1-hour) and delayed (3-hour) postexercise. *J Nucl Med* 1991;32:1961–1965.
11. Villanueva-Meyer J, Mena I, Diggles L, Narahara KA. Assessment of myocardial perfusion defect size after early and delayed SPECT imaging with

technetium-99m-hexakis 2-methoxyisobutyl isonitrile after stress. *J Nucl Med* 1993;34:187–192.
12. Dilsizian V, Arrighi JA, Diodati JG, et al. Myocardial viability in patients with chronic coronary artery disease. Comparison of ^{99m}Tc-sestamibi with thallium reinjection and [^{18}F]fluorodeoxyglucose. *Circulation* 1994;89:578–587.
13. Cuocolo A, Soricelli A, Pace L, et al. Adenosine technetium-99m methoxy isobutyl isonitrile myocardial tomography in patients with coronary artery disease: comparison with exercise. *J Nucl Med* 1994;35:1110–1115.
14. Borrello JA, Clinthorne NH, Rogers WL, Thrall JH, Keyes JW. Oblique-angle tomography: a reconstructing algorithm for transaxial tomographic data. *J Nucl Med* 1981;22:471–473.
15. Sawada SG, Allman KC, Muzik O, et al. Positron emission tomography detects evidence of viability in rest technetium-99m sestamibi defects. *J Am Coll Cardiol* 1994;23:92–98.
16. Rocco TP, Dilsizian V, Strauss HW, Boucher CA. Technetium-99m isonitrile myocardial uptake at rest. II. Relation to clinical markers of potential viability. *J Am Coll Cardiol* 1989;14:1678–1684.
17. Maurea S, Cuocolo A, Soricelli A, et al. Enhanced detection of viable myocardium by technetium-99m methoxy isobutyl isonitrile tomography after nitrates administration in patients with chronic coronary artery disease. *J Nucl Med* 1945;36:1945–1952.
18. Henry WL, De Maria A, Feigenbaum H, et al. Report of the American Society of Echocardiography Committee on nomenclature and standards: Identification of Myocardial Wall Segments. American Society of Echocardiography, November 1982, North Carolina: Duke University Medical Center.
19. Shiller NB, Shah PM, Crawford M, et al. American Society of Echocardiography Committee on Standards, Subcommittee on Quantitation of Two-dimensional Echocardiograms: recommendations for quantitation of the left ventricle by two-dimensional echocardiography. *J Am Soc Echo* 1989;2:358–367.
20. Pozzoli MMA, Fioretti PM, Salustri A, Reijis AEM, Roelandt JRTC. Exercise echocardiography and technetium-99m MIBI single-photon emission computed tomography in the detection of coronary artery disease. *Am J Cardiol* 1991;67:350–355.
21. Marzullo P, Parodi O, Reisenhofer B, et al. Value of rest thallium-201/technetium-99m sestamibi scans and dobutamine echocardiography for detecting myocardial viability. *Am J Cardiol* 1993;71:166–172.
22. Matthews DE, Farewell V. Data analysis. A formal discussion of multiple comparisons. In: *Using and understanding medical statistics*. Basel: Karger S; 1985:169–172.
23. Cuocolo A, Pace L, Ricciardelli B, Chiariello M, Trimarco B, Salvatore M. Identification of viable myocardium in patients with chronic coronary artery disease: comparison of thallium-201 scintigraphy with reinjection and technetium-99m-methoxyisobutyl isonitrile. *J Nucl Med* 1992;33:505–511.
24. Marzullo P, Sambuceti G, Parodi O. The role of sestamibi scintigraphy in the radioisotopic assessment of myocardial viability. *J Nucl Med* 1992;33:1925–1930.
25. Altehoefer C, Kaiser HJ, Dorr R, et al. Fluorine-18-deoxyglucose PET for assessment of viable myocardium in perfusion defects in Tc-99m-MIBI SPECT: a comparative study in patients with coronary artery disease. *Eur J Nucl Med* 1992;19:334–342.
26. Dondi M, Tartagni F, Fallani F, et al. A comparison of rest sestamibi and rest-redistribution thallium single photon emission tomography: possible implications for myocardial viability detection in infarcted patients. *Eur J Nucl Med* 1993;20:26–31.
27. Maurea S, Cuocolo A, Pace L, et al. Rest-injected thallium-201 redistribution and resting technetium-99m methoxy isobutyl isonitrile uptake in coronary artery disease: relation to the severity of coronary artery stenosis. *Eur J Nucl Med* 1993;20:502–510.
28. Cuocolo A, Maurea S, Pace L, et al. Resting technetium-99m-methoxy isobutyl isonitrile cardiac imaging in chronic coronary artery disease: comparison with rest-redistribution thallium-201 scintigraphy. *Eur J Nucl Med* 1993;20:1186–1192.
29. Maurea S, Cuocolo A, Pace L, et al. Left ventricular dysfunction in coronary artery disease: comparison between rest-redistribution thallium-201 and resting technetium-99m-methoxy isobutyl isonitrile cardiac imaging. *J Nucl Cardiol* 1994;1:65–71.
30. Maurea S, Cuocolo A, Nicolai E, Salvatore M. Improved detection of viable myocardium by thallium-201 reinjection in chronic coronary artery disease: comparison with technetium-99m-MIBI imaging *J Nucl Med* 1994;35:621–624.
31. Altehoefer C, vom Dahl J, Biedermann M, et al. Significance of defect severity in technetium-99m-MIBI SPECT at rest to assess myocardial viability: comparison with fluorine-18-FDG PET. *J Nucl Med* 1994;35:569–574.
32. Udelson JE, Coleman PS, Metherall J, et al. Predicting recovery of severe regional ventricular dysfunction. Comparison of resting scintigraphy with Tl-201 and Tc-99m sestamibi. *Circulation* 1994;89:2552–2561.
33. Bonow RO, Dilsizian V, Cuocolo A, Bacharach SL. Identification of viable myocardium in patients with chronic coronary artery disease and left ventricular dysfunction. Comparison of thallium scintigraphy with reinjection and PET imaging with ^{18}F-fluorodeoxyglucose. *Circulation* 1991;83:26–37.
34. Dilsizian V, Perrone-Filardi P, Arrighi JA, et al. Concordance and discordance between stress-redistribution-reinjection and rest-redistribution thallium imaging for assessing viable myocardium. Comparison with metabolic activity by positron emission tomography. *Circulation* 1993;88:941–952.
35. Kiat H, Berman DS, Maddahi J, et al. Late reversibility of tomographic myocardial thallium-201 defects. An accurate marker of myocardial viability. *J Am Coll Cardiol* 1988;12:1456–1463.
36. Kayden DS, Sigal S, Soufer R, Mattera J, Zaret BL, Wackers FJ. Thallium-201 for assessment of myocardial viability: quantitative comparison of 24-hour redistribution imaging with imaging after reinjection at rest. *J Am Coll Cardiol* 1991;18:1480–1486.
37. Dilsizian V, Smeltzer WR, Freedman NMT, Dextras R, Bonow RO. Thallium reinjection after stress-redistribution imaging. Does 24-hour delayed imaging after reinjection enhance detection of viable myocardium? *Circulation* 1991;83:1247–1255.
38. Mori T, Minamiji K, Kurogane H, Ogawa K, Yoshida Y. Rest-injected thallium-201 imaging for assessing viability of severe asynergic regions. *J Nucl Med* 1991;32:1718–1724.
39. Ragosta M, Beller GA, Watson DD, Kaul S, Gimple LW. Quantitative planar rest-redistribution Tl-201 imaging in detection of myocardial viability and prediction of improvement in left ventricular function after coronary bypass surgery in patients with severely depressed left ventricular function. *Circulation* 1993;87:1630–1641.
40. Altehoefer C, vom Dahl J, Buell U, Uebis R, Kleinhans E, Hanrath P. Comparison of thallium-201 single-photon emission tomography after rest injection and fluorodeoxyglucose positron emission tomography for assessment of myocardial viability in patients with chronic coronary artery disease. *Eur J Nucl Med* 1994;21:37–45.
41. Braunwald E, Rutherford JD. Reversible ischemic left ventricular dysfunction: evidence for "hibernating" myocardium. *J Am Coll Cardiol* 1986;8:1467–1470.